

ANALYSIS OF DISCONTINUITIES IN FLUID–SATURATED MEDIA

Marie-Angèle Abellan¹, René de Borst^{2,3} and Jean-Michel Bergheau¹

¹ LTDS-ENISE - UMR CNRS 5513, Ecole Nationale d'Ingénieurs de Saint-Etienne, F-42023 Saint-Etienne, France,

² Faculty of Aerospace Engineering, Delft University of Technology, NL-2600 GB Delft, The Netherlands,

³ LaMCoS - UMR CNRS 5514, I.N.S.A. de Lyon, F-69021 Villeurbanne, France

ABSTRACT

A finite element formulation is proposed that is capable of rigorously capturing a discontinuity in a fluid–saturated medium. It is based on the partition-of-unity property of finite element shape functions. A Heaviside distribution function is added to the displacement field and to the pressure field. The physical interpretation is discussed.

1 INTRODUCTION

Failure in elasto-plastic materials involves three distinct phases. First, a relatively large area in the body plastifies. Near the peak load, further plastic straining localises in an area of limited size. In this zone, shear strains accumulate, while in the remainder of the body elastic unloading takes place. In the third phase, progressive sliding takes place along a relatively thin zone.

To arrive at mesh–objective numerical simulations, enriched or viscous plasticity models are required for the second phase of the simulation process [1]. In case of a fluid–saturated medium, the fluid may also have a regularising effect, especially for mode–I behaviour [2].

The second phase, where the failure process is described by a regularised or viscous continuum model, should be followed by a truly discontinuous description to accommodate for gross sliding. A finite element methodology that is capable of handling this requirement can be constructed by exploiting the partition-of-unity property of finite element shape functions [3]. This concept enables the standard polynomial basis functions to be locally enriched by functions that make the element suitable for carrying out a specific task. In Belytschko *et al.* [4,5] and Wells *et al.* [6–8] Heaviside distribution functions have been chosen in order to capture a discontinuity in a displacement field.

In this contribution the concept is broadened to fluid-saturated materials. First, the governing equations are recalled for a standard biphasic material model without discontinuities. Next, the kinematic assumptions are stated as well as the assumptions regarding the constitutive behaviour in the bulk material and in the interface. A formulation is chosen for the fluid that is compatible with the assumptions for the skeleton and the physical interpretation of the consequences of this assumption is discussed. An important feature is that the constitutive behaviour of the solid grains inside the band can be different from that outside the band, while the same holds for the permeability. The ensuing equations are cast into a weak format using a Bubnov–Galerkin approach and exploiting the partition-of-unity property of the standard finite element shape functions to accommodate for the discontinuity.

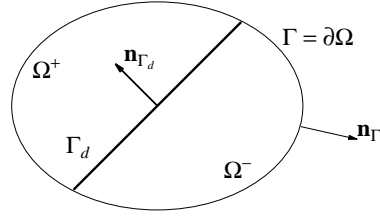


Figure 1: Body composed of continuous displacement and pressure fields \mathbf{u} and p at each side of the discontinuity Γ_d

2 STANDARD BIPHASIC MEDIUM

As point of departure we assume a standard biphasic medium subjected the restriction of small displacement gradients. In the same spirit, the variations of the concentrations are assumed to be small. Furthermore, the assumption is made that the grains are incompressible. With these assumptions and neglecting inertia forces, the balances of momentum and mass read, respectively:

$$\nabla \cdot \boldsymbol{\sigma} = \mathbf{0} \quad (1)$$

with $\boldsymbol{\sigma}$ the stress tensor of the total medium, and

$$\nabla \cdot \dot{\mathbf{u}} + \nabla \cdot (n_f \mathbf{w}_f) + Q^{-1} \dot{p} = 0 \quad (2)$$

with \mathbf{w}_f the fluid velocity relative to the velocity of the skeleton $\dot{\mathbf{u}}$, n_f the fluid volumic fraction, p the fluid pressure and

$$Q^{-1} = \frac{1 - n_f}{K_s} + \frac{n_f}{K_f} \quad (3)$$

with K_s and K_f the bulk moduli of the skeleton and the fluid, respectively. The governing equations (1) and (2) together with the boundary conditions

$$\boldsymbol{\sigma} \cdot \mathbf{n}_\Gamma = \mathbf{t}_p \quad , \quad \mathbf{u} = \mathbf{u}_p \quad (4)$$

on complementary parts of the boundary $\partial\Omega_t$ and $\partial\Omega_u$, with $\Gamma = \partial\Omega = \partial\Omega_t \cup \partial\Omega_u$ and $\partial\Omega_t \cap \partial\Omega_u = \emptyset$, and

$$n_f \mathbf{w}_f = \mathbf{q}_p \quad , \quad p = p_p \quad (5)$$

on complementary parts of the boundary $\partial\Omega_q$ and $\partial\Omega_p$, with $\Gamma = \partial\Omega = \partial\Omega_q \cup \partial\Omega_p$ and $\partial\Omega_q \cap \partial\Omega_p = \emptyset$, \mathbf{n}_Γ being the outward unit normal on the external boundary, Figure 1, and \mathbf{t}_p the prescribed external traction and the subscript p denoting prescribed quantities.

3 KINEMATICS AND CONSTITUTIVE ASSUMPTIONS

A displacement field \mathbf{u} that contains a single discontinuity at $\partial\Omega_d = \Gamma_d$ can be written as the sum of two continuous displacement fields $\bar{\mathbf{u}}$ and $\tilde{\mathbf{u}}$ separated by a Heaviside function \mathcal{H}_{Γ_d} :

$$\mathbf{u}(\mathbf{x}, t) = \bar{\mathbf{u}}(\mathbf{x}, t) + \mathcal{H}_{\Gamma_d} \tilde{\mathbf{u}}(\mathbf{x}, t) \quad (6)$$

Using eqn (6) the strain field follows by straightforward differentiation:

$$\boldsymbol{\epsilon} = \nabla^s \bar{\mathbf{u}} + \mathcal{H}_{\Gamma_d} \nabla^s \tilde{\mathbf{u}} + \delta_{\Gamma_d} (\tilde{\mathbf{u}} \otimes \mathbf{n}_{\Gamma_d})^s \quad (7)$$

where the superscript s denotes a symmetrised operator and δ_{Γ_d} is the Dirac function placed at the discontinuity Γ_d . For notational simplicity, the explicit dependence of the various quantities and fields on \mathbf{x} and t has been dropped.

We now consider the case that a diaphragm with a permeability k_d is placed at the discontinuity in the displacements. As a consequence, the fluid pressure can be discontinuous across Γ_d and, similar to eqn (6), we have:

$$p(\mathbf{x}, t) = \bar{p}(\mathbf{x}, t) + \mathcal{H}_{\Gamma_d} \tilde{p}(\mathbf{x}, t) \quad (8)$$

It is noted that this assumption is different from that of Armero and Callari [9], who adopt a smooth pressure field (and therefore $p = \bar{p}$) and also different from that of Larsson and Larsson [10], who assume that a regularised Dirac distribution is added to the continuous pressure field at the location of the discontinuity in the displacement field. For the fluid flow, gradients of the pressure need to be computed. Differentiating eqn (8), we obtain:

$$\nabla p = \nabla \bar{p} + \mathcal{H}_{\Gamma_d} \nabla \tilde{p} + \delta_{\Gamma_d} \tilde{p} \mathbf{n}_{\Gamma_d} \quad (9)$$

where, similar to eqn (7), the explicit dependence on \mathbf{x} and t has been dropped for notational simplicity.

The above kinematics have to be complemented by constitutive equations to be inserted in the weak form of the balance equations for momentum and mass. The solid phase is assumed to be inviscid and ‘simple’ in the sense of Noll and moreover, assumed to obey an incremental-linear constitutive relation. Thus, for the bulk material we have, following the assumption of an incremental-linear solid, the following form of the constitutive equation:

$$d\boldsymbol{\sigma}_s = \mathbf{D} : d\boldsymbol{\epsilon} \quad (10)$$

with \mathbf{D} denoting the tangential material tensor in the bulk material, and $\boldsymbol{\sigma}_s$ the stress tensor in the skeleton of the bulk:

$$\boldsymbol{\sigma}_s = \boldsymbol{\sigma} + p\mathbf{I} \quad (11)$$

The d -symbol denotes an infinitesimally small variation of a quantity. Inserting the stress decomposition (11) together with the decompositions (6) and (8) into the constitutive relation (10), one obtains:

$$d\boldsymbol{\sigma} = \mathbf{D} : (\nabla^s d\bar{\mathbf{u}} + \mathcal{H}_{\Gamma_d} \nabla^s d\tilde{\mathbf{u}}) - (d\bar{p} + \mathcal{H}_{\Gamma_d} d\tilde{p})\mathbf{I} \quad (12)$$

since the Dirac function vanishes away from the discontinuity. Assuming that the fluid flow in the porous medium can be described sufficiently accurately by Darcy’s relation,

$$\mathbf{w}_f = -\frac{k_f}{n_f} \nabla p \quad (13)$$

k_f being the permeability of the bulk material, the behaviour of the bulk of the fluid-saturated medium is completely captured.

In the spirit of eqn (10) a tangential interface relation is also postulated between the interface tractions \mathbf{t}_d and the relative displacements $\mathbf{v} = \tilde{\mathbf{u}}|_{\mathbf{x} \in \Gamma_d}$:

$$d\mathbf{t}_d = \mathbf{T} \cdot d\mathbf{v} \quad (14)$$

Similarly, a discrete equivalent of Darcy’s relation for the fluid flow \mathbf{q}_d at the interface can be defined as

$$\mathbf{n}_{\Gamma_d} \cdot \mathbf{q}_d = -k_d(p^+ - p^-) = -k_d \tilde{p}|_{\mathbf{x} \in \Gamma_d} \quad (15)$$

where it is recalled that k_d is the permeability of the diaphragm that is thought to coincide with the displacement discontinuity Γ_d and p^+ and p^- are the pressures in the Ω^+ and Ω^- domains, respectively. Evidently, for an impervious boundary, one has $k_d = 0$, which, according to eqn (15), implies that $\mathbf{n}_{\Gamma_d} \cdot \mathbf{q}_d = 0$. Conversely, ideal permeability requires that $k_d \rightarrow \infty$, so that the term can only be bounded if $p^+ - p^- = 0$, which implies that no discontinuity can exist in the pressure field and the formulation of Armero and Callari [9] is retrieved.

It is noted that another boundary condition for the fluid flow can be formulated at the internal boundary Γ_d :

$$\mathbf{n}_{\Gamma_d} \cdot \mathbf{q}_d = q_d \quad |_{\mathbf{x} \in \Gamma_d} \quad (16)$$

Such a boundary condition would represent the existence of a drain (or a line source) with a capacity q_d per unit length.

4 WEAK FORMAT AND DISCRETISATION

In the spirit of a standard Bubnov–Galerkin approach, we assume test functions for the displacements and the pressures as:

$$\boldsymbol{\eta} = \bar{\boldsymbol{\eta}} + \mathcal{H}_{\Gamma_d} \tilde{\boldsymbol{\eta}} \quad (17)$$

and

$$\zeta = \bar{\zeta} + \mathcal{H}_{\Gamma_d} \tilde{\zeta} \quad (18)$$

Substitution into eqns (1)–(2) and integrating over the domain Ω leads to the corresponding weak forms:

$$\int_{\Omega} (\bar{\boldsymbol{\eta}} + \mathcal{H}_{\Gamma_d} \tilde{\boldsymbol{\eta}}) \cdot \nabla \cdot \boldsymbol{\sigma} d\Omega = 0 \quad (19)$$

and

$$\int_{\Omega} (\bar{\zeta} + \mathcal{H}_{\Gamma_d} \tilde{\zeta}) [\nabla \cdot \dot{\mathbf{u}} + \nabla \cdot (n_f \mathbf{w}_f) + Q^{-1} \dot{p}] d\Omega = 0 \quad (20)$$

We next apply the divergence theorem, use the external boundary conditions (4) and (5), eliminate the Heaviside functions by changing the integration domain from Ω to Ω^+ and eliminate the Dirac functions by transforming the volume integral into a surface integral:

$$\int_{\Omega} \nabla \bar{\boldsymbol{\eta}} : \boldsymbol{\sigma} d\Omega + \int_{\Omega^+} \nabla \tilde{\boldsymbol{\eta}} : \boldsymbol{\sigma} d\Omega + \int_{\Gamma_d} \tilde{\boldsymbol{\eta}} \cdot \mathbf{t}_d d\Omega = \int_{\Gamma} (\bar{\boldsymbol{\eta}} + \mathcal{H}_{\Gamma_d} \tilde{\boldsymbol{\eta}}) \cdot \mathbf{t}_p d\Omega \quad (21)$$

and

$$\begin{aligned} & - \int_{\Omega} \bar{\zeta} \nabla \cdot \dot{\mathbf{u}} d\Omega - \int_{\Omega^+} \tilde{\zeta} \nabla \cdot \dot{\mathbf{u}} d\Omega + \int_{\Omega} \nabla \bar{\zeta} \cdot (n_f \mathbf{w}_f) d\Omega + \int_{\Omega^+} \nabla \tilde{\zeta} \cdot (n_f \mathbf{w}_f) d\Omega \\ & + \int_{\Gamma_d} \tilde{\zeta} \mathbf{n}_{\Gamma_d} \cdot \mathbf{q}_d d\Gamma - \int_{\Omega} \bar{\zeta} Q^{-1} \dot{p} d\Omega - \int_{\Omega^+} \tilde{\zeta} Q^{-1} \dot{p} d\Omega = \int_{\Gamma} (\bar{\zeta} + \mathcal{H}_{\Gamma_d} \tilde{\zeta}) \mathbf{n}_{\Gamma} \cdot \mathbf{q}_p d\Gamma \end{aligned} \quad (22)$$

where $\mathbf{t}_d = \boldsymbol{\sigma} \cdot \mathbf{n}_{\Gamma_d}$ is the traction at the discontinuity.

In a Bubnov–Galerkin sense the trial functions \mathbf{u} and p and the test functions $\boldsymbol{\eta}$ and ζ are discretised in the same space:

$$\mathbf{u} = \mathbf{N}(\bar{\mathbf{a}} + \mathcal{H}_{\Gamma_d} \tilde{\mathbf{a}}) \quad , \quad p = \mathbf{H}(\bar{\mathbf{p}} + \mathcal{H}_{\Gamma_d} \tilde{\mathbf{p}}) \quad (23)$$

$$\boldsymbol{\eta} = \mathbf{N}(\bar{\mathbf{w}} + \mathcal{H}_{\Gamma_d} \tilde{\mathbf{w}}) \quad , \quad \zeta = \mathbf{H}(\bar{\mathbf{z}} + \mathcal{H}_{\Gamma_d} \tilde{\mathbf{z}}) \quad (24)$$

where the partition-of-unity property of the shape functions contained in \mathbf{N} and \mathbf{H} has been exploited. The arrays $\bar{\mathbf{a}}$ and $\bar{\mathbf{p}}$ contain the nodal values of the underlying continuous fields $\bar{\mathbf{u}}$ and \bar{p} ,

while the arrays $\tilde{\mathbf{a}}$ and $\tilde{\mathbf{p}}$ contain the nodal values of the underlying continuous fields $\tilde{\mathbf{u}}$ and \tilde{p} . The arrays $\tilde{\mathbf{w}}$, $\tilde{\mathbf{z}}$, $\tilde{\mathbf{w}}$ and $\tilde{\mathbf{z}}$ contain the discrete values related to the respective test functions. Inserting eqns (24) into eqns (22) and (21) and requiring that the result holds for all admissible $\tilde{\mathbf{w}}$, $\tilde{\mathbf{z}}$, $\tilde{\mathbf{w}}$ and $\tilde{\mathbf{z}}$ gives, using the standard notation $\mathbf{B} = \mathbf{LN}$:

$$\int_{\Omega} \mathbf{B}^T \boldsymbol{\sigma} d\Omega = \int_{\Gamma} \mathbf{N}^T \mathbf{t}_p d\Gamma \quad (25)$$

$$\int_{\Omega^+} \mathbf{B}^T \boldsymbol{\sigma} d\Omega + \int_{\Gamma_d} \mathbf{N}^T \mathbf{t}_d d\Gamma = \int_{\Gamma} \mathcal{H}_d \mathbf{N}^T \mathbf{t}_p d\Gamma \quad (26)$$

$$- \int_{\Omega} \mathbf{H}^T \mathbf{m}^T \dot{\mathbf{u}} d\Omega + \int_{\Omega} \nabla \mathbf{H}^T n_f \mathbf{w}_f d\Omega - \int_{\Omega} \mathbf{H}^T Q^{-1} \dot{p} d\Omega = \int_{\Gamma} \mathbf{H}^T \mathbf{n}_{\Gamma_d}^T \mathbf{q}_p d\Gamma \quad (27)$$

$$\begin{aligned} - \int_{\Omega^+} \mathbf{H}^T \mathbf{m}^T \dot{\mathbf{u}} d\Omega + \int_{\Omega^+} \nabla \mathbf{H}^T n_f \mathbf{w}_f d\Omega - \int_{\Omega^+} \mathbf{H}^T Q^{-1} \dot{p} d\Omega + \int_{\Gamma_d} \mathbf{H}^T \mathbf{n}_{\Gamma_d}^T \mathbf{q}_d d\Gamma \\ = \int_{\Gamma} \mathcal{H}_d \mathbf{H}^T \mathbf{n}_{\Gamma_d}^T \mathbf{q}_p d\Gamma \end{aligned} \quad (28)$$

with $\mathbf{m}^T = (1, 1, 1, 0, 0, 0)$.

For using the Newton-Raphson method to solve eqns (25)–(28) they have to be linearised. To this end, the stress and the pressure are decomposed as follows

$$\boldsymbol{\sigma}_j = \boldsymbol{\sigma}_{j-1} + d\boldsymbol{\sigma} \quad , \quad p_j = p_{j-1} + dp \quad (29)$$

with the subscripts $j - 1$ and j signifying the iteration numbers. Substituting these decompositions into the discrete set of equations (25)–(28), utilising the kinematic relation (7), the stress–strain relation (12) for the bulk material and the traction–relative displacement relation (14) at the interface, using Darcy’s relation for the fluid flow in the porous medium (13), its discrete equivalent (15) at the interface and the expression (9) for the pressure gradient and using the interpolations for the displacement and the pressure according to eqns (23), leads to the following set of equations linearised at iteration $j - 1$:

$$\begin{aligned} \begin{bmatrix} \mathbf{0} & \mathbf{0} & \mathbf{0} & \mathbf{0} \\ \mathbf{0} & \mathbf{0} & \mathbf{0} & \mathbf{0} \\ \mathbf{K}_{\bar{a}\bar{p}}^T & \mathbf{K}_{\bar{a}\bar{p}}^T & \mathbf{K}_{\bar{p}\bar{p}}^{(1)} & \mathbf{K}_{\bar{p}\bar{p}}^{(1)} \\ \mathbf{K}_{\bar{a}\bar{p}}^T & \mathbf{K}_{\bar{a}\bar{p}}^T & \mathbf{K}_{\bar{p}\bar{p}}^{(1)} & \mathbf{K}_{\bar{p}\bar{p}}^{(1)} \end{bmatrix} \begin{pmatrix} \dot{\bar{\mathbf{a}}} \\ \dot{\bar{\mathbf{a}}} \\ \dot{\bar{\mathbf{p}}} \\ \dot{\bar{\mathbf{p}}} \end{pmatrix} + \begin{bmatrix} \mathbf{K}_{\bar{a}\bar{a}} & \mathbf{K}_{\bar{a}\bar{a}} & \mathbf{K}_{\bar{a}\bar{p}} & \mathbf{K}_{\bar{a}\bar{p}} \\ \mathbf{K}_{\bar{a}\bar{a}} & \mathbf{K}_{\bar{a}\bar{a}} & \mathbf{K}_{\bar{a}\bar{p}} & \mathbf{K}_{\bar{a}\bar{p}} \\ \mathbf{0} & \mathbf{0} & \mathbf{K}_{\bar{p}\bar{p}}^{(2)} & \mathbf{K}_{\bar{p}\bar{p}}^{(2)} \\ \mathbf{0} & \mathbf{0} & \mathbf{K}_{\bar{p}\bar{p}}^{(2)} & \mathbf{K}_{\bar{p}\bar{p}}^{(2)} \end{bmatrix} \begin{pmatrix} d\bar{\mathbf{a}}_j \\ d\bar{\mathbf{a}}_j \\ d\bar{\mathbf{p}}_j \\ d\bar{\mathbf{p}}_j \end{pmatrix} \\ = \begin{pmatrix} \mathbf{f}_{\bar{a}}^{ext} - \mathbf{f}_{\bar{a},j-1}^{int} \\ \mathbf{f}_{\bar{a}}^{ext} - \mathbf{f}_{\bar{a},j-1}^{int} \\ \mathbf{f}_{\bar{p}}^{ext} - \mathbf{f}_{\bar{p},j-1}^{int} \\ \mathbf{f}_{\bar{p}}^{ext} - \mathbf{f}_{\bar{p},j-1}^{int} \end{pmatrix} \end{aligned} \quad (30)$$

with $\mathbf{f}_{\bar{a}}^{ext}$ $\mathbf{f}_{\bar{p}}^{ext}$ given by the right-hand sides of eqns (25)–(28), respectively, with $\mathbf{f}_{\bar{a}}^{int}$ $\mathbf{f}_{\bar{p}}^{int}$ given by the left-hand sides of eqns (25)–(28), and with the stiffness matrices defined as:

$$\mathbf{K}_{\bar{a}\bar{a}} = \int_{\Omega} \mathbf{B}^T \mathbf{D} \mathbf{B} d\Omega \quad , \quad \mathbf{K}_{\bar{a}\bar{a}} = \int_{\Omega^+} \mathbf{B}^T \mathbf{D} \mathbf{B} d\Omega \quad (31)$$

$$\mathbf{K}_{\bar{a}\bar{a}} = \int_{\Omega^+} \mathbf{B}^T \mathbf{D} \mathbf{B} d\Omega + \int_{\Gamma_d} \mathbf{N}^T \mathbf{T} \mathbf{N} d\Gamma \quad (32)$$

$$\mathbf{K}_{\bar{a}\bar{p}} = - \int_{\Omega} \mathbf{B}^T \mathbf{m} \mathbf{H} d\Omega \quad , \quad \mathbf{K}_{\bar{a}\bar{p}} = - \int_{\Omega^+} \mathbf{B}^T \mathbf{m} \mathbf{H} d\Omega \quad (33)$$

$$\mathbf{K}_{\bar{p}\bar{p}}^{(1)} = - \int_{\Omega} \mathbf{H}^T Q^{-1} \mathbf{H} d\Omega \quad , \quad \mathbf{K}_{\bar{p}\bar{p}}^{(1)} = - \int_{\Omega^+} \mathbf{H}^T Q^{-1} \mathbf{H} d\Omega \quad (34)$$

$$\mathbf{K}_{\bar{p}\bar{p}}^{(2)} = - \int_{\Omega} \nabla \mathbf{H}^T k_f \nabla \mathbf{H} d\Omega \quad , \quad \mathbf{K}_{\bar{p}\bar{p}}^{(2)} = - \int_{\Omega^+} \nabla \mathbf{H}^T k_f \nabla \mathbf{H} d\Omega \quad (35)$$

$$\mathbf{K}_{\bar{p}\bar{p}}^{(2)} = - \int_{\Omega^+} \nabla \mathbf{H}^T k_f \nabla \mathbf{H} d\Omega - \int_{\Gamma_d} \mathbf{H}^T k_d \mathbf{H} d\Gamma \quad (36)$$

For the time integration of eq. (30), the reader is referred to de Borst *et al.* [11].

5 CONCLUDING REMARKS

The partition-of-unity property of finite element shape functions has been exploited to describe discontinuities in fluid-saturated media (cracks, shear bands). Attention has been paid to the modelling of the fluid behaviour at the interface. The ensuing equations have been elaborated in a finite element context.

REFERENCES

1. de Borst R. Some recent issues in computational failure mechanics, *Int. J. Num. Meth. Eng.* 52, 63–95, 2001.
2. Schrefler BA, Sanavia L, Majorana CE. A multiphase medium model for localisation and postlocalisation simulation in geomaterials, *Mech. Cohes.-frict. Mater.* 1, 95–114, 1996.
3. Babuska I, Melenk JM. The partition of unity method, *Int. J. Num. Meth. Eng.* 40, 727-758, 1997.
4. Belytschko T, Black T. Elastic crack growth in finite elements with minimal remeshing, *Int. J. Num. Meth. Eng.* 45, 601–620, 1999.
5. Moës N, Dolbow J, Belytschko T. A finite element method for crack growth without remeshing, *Int. J. Num. Meth. Eng.* 46, 131–150, 1999.
6. Wells GN, Sluys LJ. A new method for modelling cohesive cracks using finite elements, *Int. J. Num. Meth. Eng.* 50, 2667–2682, 2001.
7. Wells GN, Sluys LJ, de Borst R. Simulating the propagation of displacement discontinuities in a regularized strain-softening medium, *Int. J. Num. Meth. Eng.* 53, 1235-1256, 2002.
8. Wells GN, de Borst R, Sluys LJ. A consistent geometrically non-linear approach for delamination, *Int. J. Num. Meth. Eng.* 54, 1333-1355, 2002.
9. Armero F, Callari C. An analysis of strong discontinuities in a saturated poro-plastic solid, *Int. J. Num. Meth. Eng.* 46, 1673–1698, 1999.
10. Larsson J, Larsson, R. Localization analysis of a fluid-saturated elastoplastic porous medium using regularized discontinuities, *Mech. Cohes.-frict. Mater.* 5, 565–582, 2000.
11. de Borst R, Remmers JJC, Needleman A, Abellan MA. Discrete vs smeared crack models for concrete fracture: Bridging the gap, *Int. J. Num. Anal. Meth. Geomech.* 28, 000–000, 2004.